Effect of Metal Cation Type on the Structure and Properties of Ethylene Ionomers

EISAKU HIRASAWA,[1,*] YOSHIMASA YAMAMOTO,[1] KENJI TADANO,[2] and SHINICHI YANO[3]

[1]Technical Center, Du Pont Mitsui Polychemicals Co. Ltd., Chigusa Kaigan 6, Ichihara, Chiba 299-01, Japan, [2]Gifu College of Medical Technology, Ichihirage, Seki, Gifu 501-32, Japan, and [3]Department of Chemistry, Faculty of Engineering, Gifu University, Yanagido, Gifu 501-11, Japan

SYNOPSIS

Thermal properties by DSC, stiffness, melt viscosity, tensile properties, and dynamic mechanical properties were measured for the Na^+, K^+, Mg^{2+}, Zn^{2+}, Cu^{2+}, Mn^{2+}, and Co^{2+} salts of poly(ethylene-*co*-methacrylic acid) (EMAA). The changes in the structure and properties with increasing neutralization are larger in the alkaline and alkaline earth metal salts than in the transition metal salts. The stiffness shows a maximum at 33% neutralization in both the alkaline and alkaline earth metal salts, while no maxima are found up to 60% neutralization in the transition metal salts. The microphase separation of salt group aggregates is observed in both the alkaline and alkaline earth metal salts, but is not seen in the transition metal salts. These differences were attributed to both the stronger ionic interactions and the larger number of carboxyl groups associated with the alkaline and alkaline earth metal salts in the ordered structure of ionic salt groups (ionic crystallites). The mechanical properties measured at low strain, such as stiffness and yield stress, strongly depend on the degree of the crystalline order of the ionic crystallites. The high-strain properties, such as tensile strength and elongation at break, depend on the strength of the ionic interactions and the valence of the cation.

INTRODUCTION

Ionomers are defined as polymers containing hydrophobic backbone chains and a small amount of ionic groups attached on the backbones, side chains, or on backbone terminals. It is generally accepted that the polar salt groups form ionic aggregations such as multiplets and clusters in the hydrophobic polymer matrix. Especially, the presence of ionic clusters has been evidenced by various techniques such as small-angle X-ray scattering (SAXS), dynamic mechanical and dielectric measurements, electron microscopy, and electron spin resonance spectroscopy (ESR).[1-8] The introduction of ionic groups onto hydrophobic backbone chains results in a dramatic increase in mechanical properties such as modulus, tensile strength, impact resistance, and, in particular, stiffness (bending modulus).[2,9-11] Ionomers have been widely used in commercial applications by taking advantage of their characteristic properties originating in the ionic interactions. Among those that are also widely recognized for ionomers are change of stiffness with physical aging after molding from melt and a considerable difference in the crystallinity and stiffness depending on thermal history.[12-15]

A large number of studies have been made on the structure of ionic aggregations and the structure–property relations. Several structural models for the ionic clusters have been proposed.[1,2,16-23] However, despite a lot of research efforts on morphological studies of the ionic clusters, not one convincing conclusion has yet been obtained. The structural mechanisms underlying both the dramatic increase in stiffness upon neutralization and the change in stiffness with aging also have not been fully clarified.

In our preceding works[24,25] on zinc (II) salts and complex zinc (II) salts with 1,3-bis(aminomethyl)-cyclohexane (BAC) of poly(ethylene-*co*-methacrylic acid) (EMAA), we obtained the following

* To whom all correspondence should be addressed.

Journal of Applied Polymer Science, Vol. 42, 351–362 (1991)
 CCC 0021-8995/91/020351-12$04.00

new and interesting results: the ionic clusters consist of ordered assemblies of ionic groups (ionic crystallites) in the solid state. The ionic clusters undergo an order–disorder transition of the first order at the transition temperature (T_i) near 330 K. Internally the ionic clusters are in a disordered state above T_i. The ionic crystallites are not formed at T_i during cooling from melt, but originate and develop gradually in a relaxation process with a long relaxation time during aging at room temperature after molding from melt. The stiffness of ionomer increases along with the development of the ionic crystallites. The origin of both the enhanced stiffness upon neutralization and the change in stiffness with aging time is the formation and buildup of the ionic crystallites. The stiffness of ionomer is closely connected with the degree of crystallinity of the ionic crystallites (heat of fusion of the ionic crystallites), and the increase in stiffness differs by the type of cation species.

Following the preceding works, this article deals with how the ionic aggregations affect the structure and properties of ethylene ionomers. The purpose of this work is to clarify how the structure, especially of the ionic crystallites, differs by the type of metal cations and how this difference affects the physical properties. For this purpose, thermal properties by differential scanning calorimetory (DSC), stiffness, tensile properties, melt flow rate, and dynamic mechanical properties were measured for the various alkaline, alkaline earth, and transition metal salts of EMAA.

EXPERIMENTAL

Materials and Sample Preparation

The samples used are represented hereafter as EMAA-xMe, where EMAA is poly(ethylene-*co*-methacrylic), x is the degree of neutralization of carboxylic acid group by metal cation, and Me is the metal cation species represented by atomic symbol. EMAA is ACR-1560 of Du Pont–Mitsui Polychemicals Co. Ltd., where methacrylic acid content is 5.4 mol %.

All ionomers were prepared by means of melt reaction of EMAA with stoichiometric quantity of cation sources in an extruder at 180–260°C. As cation sources, Na_2CO_3, K_2CO_3, $Mg(OH)_2$, ZnO, $Cu(CH_3COO)_2$, $Mn(CH_3COO)_2 \cdot 4H_2O$ and $Co(CH_3COO)_2$ were used. Volatile by-products such as H_2O, CO_2, and CH_3COOH resulting from the neutralization were eliminated at a vacuum extraction port equipped on the extruder. Melt strands from the extruder die were cooled in water and were pelletized. Melt strands from the extruder die were transparent for all ionomers, which means the reaction proceeded stoichiometrically. If the reaction is incomplete, the strands are opaque or translucent. The pellet samples were dryed and stored in moisture barrier bags at room temperature in order to prevent moisture pickup.

The pellet samples were compression molded into sheets of 2 or 3 mm thickness at 5 MPa and 160°C. These sheet samples were then cooled to room temperature in 5 min at 5 MPa using a cooling rate of about 30°C/min. This was accomplished by placing the molding in a press maintained at 20°C. The sheet samples were aged in moisture barrier bags at room temperature (18–23°C) until the measurements were made.

Measurements

Melt flow rate (MFR) was measured as weight of flow in grams per 10 min from a melt indexer at 190°C and under 2160-g load.

Differential scanning calorimetric (DSC) measurements were conducted on 10-mg specimens at a heating/cooling rate of 10°C/min. using a DuPont DSC-990 calorimeter. The specimens used for DSC were prepared as follows: for Na, K, Mg, and Zn ionomers and EMAA, the specimens were taken from the compression-molded sheets aged for 2 months at room temperature after the molding; for Cu, Mn, and Co ionomers, the specimens were taken from pellet samples aged for 30 days. The melting point and heat of fusion for both ionic and polyethylene crystallites were obtained from the peak temperature and peak area of the endothermic peak, respectively, on DSC thermograms in the first heating process. Crystallization temperature of the polyethylene region was obtained from the peak temperature of the exothermic peak in the cooling process. Indium was used as a calibration standard.

Stiffness (bending modulus) was measured at 23°C for a slab (20 mm wide × 100 mm long × 3 mm thick) stamped out from the compression-molded sheets, according to ASTM D-747. Specimen stiffness was measured at various aging durations after the molding. Aging durations for each ionomer were as follows: Zn ionomer and EMAA—9 days, 2 months, 3 months; Na, K, and Mg ionomer—2 months, 3 months; Cu, Mn, and Co ionomer—9 days.

Tensile properties were measured on dogbone samples stamped out from 2-mm-thick compression-molded sheets aged for a month at room temperature

after the molding. Measurements were performed at 23°C and at a crosshead speed of 200 mm/min using a Shimadzu Autograph DSC-R-100.

Dynamic mechanical measurements were conducted for a slab (40 mm long × 12 mm wide × 3 mm thick) in a temperature range from −150 to 80°C, and at a heating rate of 5°C/min using a DuPont 982DMA. Here, the oscillation mode produced by dynamic stress imposed on a sample retains a constant amplitude of 0.2 mm. Frequency varied between 2 and 20 Hz depending on the modulus.

RESULTS AND DISCUSSION

Table I lists DSC thermal data for all samples. Table II shows rheological and physical properties of the samples.

Melting, Crystallization, and Crystallinity of Ionic and Polyethylene Crystallites Measured by DSC

Figure 1 shows how DSC thermograms vary with the degree of neutralization for Zn ionomers that

Table I DSC Thermal Data of All Ionomers

	DSC Thermal Data								
	First Heating					Second Heating			Cooling
	Ionic Cryst.		PE Cryst.			PE Cryst.			PE Cryst.
Sample Designation	T_i[a] (°C)	ΔH_i[b] (mJ/mg)	T_m[c] (°C)	ΔH_m[d] (mJ/mg)	% Cryst.[e] (%)	T_m (°C)	ΔH_m (mJ/mg)	% Cryst. (%)	T_c[f] (°C)
EMAA	42	5.3	92	61.6	21				65
EMAA–0.2 Na	45	7.9	92	67.0	23	92	65.8	23	62
EMAA–0.4 Na	48	9.4	91	45.3	16	91	48.3	17	52
EMAA–0.6 Na	50	13.7	89	36.7	13	88	28.7	10	46
EMAA–0.8 Na	50	11.8	89	26.8	9.2	86	17.2	5.9	42
EMAA–0.9 Na	54	13.3	87	23.5	8.1	86	14.4	5.0	42
EMAA–0.2 K	45	6.9	92	61.4	21	92	62.7	22	65
EMAA–0.4 K	47	10.8	92	54.0	19	91	55.8	19	57
EMAA–0.6 K	54	15.6	89	32.2	11	89	33.8	12	46
EMAA–0.2 Mg	51	12.5	91	55.6	19	91	54.7	19	55
EMAA–0.4 Mg	56	14.2	89	38.1	13	89	36.1	12	47
EMAA–0.6 Mg	57	16.5	87	21.6	7.4	86	24.6	8.5	42
EMAA–0.8 Mg	56	14.5	84	14.7	5.1	84	9.8	3.4	37
EMAA–0.9 Mg	58	12.6	84	11.4	3.9	85	8.3	2.9	37
EMAA–0.2 Zn	46	8.3	91	67.9	23	91	64.5	22	64
EMAA–0.4 Zn	48	9.2	91	56.3	19	90	54.4	19	61
EMAA–0.6 Zn	50	9.6	90	57.3	20	88	47.6	16	58
EMAA–0.8 Zn	52	11.7	88	46.0	16	87	38.9	13	51
EMAA–0.9 Zn	53	13.1	88	42.3	15	87	37.0	13	51
EMAA–0.2 Cu	49	10.0	92	60.3	21	91			69
EMAA–0.4 Cu	51	11.5	91	56.1	19	92			68
EMAA–0.6 Cu	55	14.3	91	51.1	18	91			60
EMAA–0.2 Mn	41	9.1	92	61.7	21	92			66
EMAA–0.4 Mn	44	9.1	93	58.2	20	93			64
EMAA–0.6 Mn	49	14.8	92	48.1	17	92			57
EMAA–0.2 Co	49	9.3	92	53.2	18	93			63
EMAA–0.4 Co	51	12.7	90	50.7	17	91			61
EMAA–0.6 Co	53	20.0	89	39.8	14	89			55

[a] Melting point of ionic crystallites.
[b] Heat of fusion of ionic crystallites.
[c] Melting point of polyethylene crystallites.
[d] Heat of fusion of polyethlene crystallites.
[e] Degree of crystallinity of polyethlene crystallites.
[f] Crystallizing point of polyethlene crystallites.

Table II Rheological and Physical Properties of the Samples

Sample Designation	MFR at 190°C (dg/min)	Stiffness (MPa) Aging Durations			Tensile Properties		
		9 Day	2 Month	3 Month	Yield Stress (MPa)	Tensile Strength (MPa)	Elongation at Break (%)
EMAA	60	70	82	83	8.2	22.0	530
EMAA–0.2 Na	18		169	196	12.9	24.6	473
EMAA–0.4 Na	4.6		277	320	16.1	30.4	387
EMAA–0.6 Na	1.0		256	325	16.0	31.5	295
EMAA–0.8 Na	0.23		245	310	18.0	34.3	324
EMAA–0.9 Na	0.18		248	309	17.2	34.0	319
EMAA–0.2 K	17		137	167	13.0	24.5	462
EMAA–0.4 K	4.7		236	238	15.3	24.4	320
EMAA–0.6 K	1.3		245	231	14.8	28.1	417
EMAA–0.2 Mg	18		191	252	14.9	25.9	439
EMAA–0.4 Mg	4.5		285	362	18.8	29.7	350
EMAA–0.6 Mg	0.80		254	321	19.2	29.0	299
EMAA–0.8 Mg	0.06		208	276	21.3	28.0	196
EMAA–0.9 Mg	0.06		205	280	20.4	21.5	72
EMAA–0.2 Zn	23	109	124	140	10.9	22.2	412
EMAA–0.4 Zn	8.7		183	235	15.8	24.9	400
EMAA–0.6 Zn	3.6	223	255	302	15.4	27.8	375
EMAA–0.8 Zn	1.0		298	343	17.9	24.2	267
EMAA–0.9 Zn	0.40		298	347	20.1	22.7	126
EMAA–0.2 Cu	23	124			10.3	22.1	452
EMAA–0.4 Cu	9.9	186			12.9	21.3	408
EMAA–0.6 Cu	5.7	243			15.7	17.6	208
EMAA–0.2 Mn	31	123					
EMAA–0.4 Mn	18	196			13.3	27.4	433
EMAA–0.6 Mn	10	278			15.8	28.2	375
EMAA–0.2 Co	16	160			21.8	24.6	437
EMAA–0.4 Co	9.8	249			16.7	17.8	121
EMAA–0.6 Co	5.2	288			17.4	17.5	95

were aged at room temperature for 2 months after the molding. At the first heating, two endothermic peaks are observed near 50 and 90°C. The higher temperature peak, whose peak temperature and heat of fusion are denoted hereafter by T_m and ΔH_m, respectively, corresponds to the melting of the polyethylene crystalline region in the polymer matrix. The lower temperature peak, whose peak temperature and heat of fusion are denoted hereafter by T_i and ΔH_i, respectively, is attributed to the order–disorder transition of a first order in ionic clusters (melting of ionic crystallites), as reported in our preceding work.[24] In the cooling process from the molten state, one exothermic peak, whose peak temperature is denoted hereafter by T_c, is observed near 60°C. This corresponds to the crystallization of the polyethylene chain. At the second heating soon after the cooling, only one peak is observed at almost the same temperature as T_m and with nearly the same heat of fusion as ΔH_m in the first heating. The lower temperature peak is suppressed in the second heating process. DSC thermograms similar to these are observed for all the metal ionomers used in this work.

Figures 2(*a*) and (*b*) show plots of T_i, T_m, and T_c versus degree of neutralization in the ionomers neutralized with various metal cations. The plots for ΔH_m and ΔH_i versus degree of neutralization are shown in Figures 3(*a*) and (*b*). In the figures, both solid marks and solid lines show the data for the alkaline and alkaline earth metal salts (Na^+, K^+, and Mg^{2+}); both open marks and dotted lines show the data for the transition metal salts (Zn^{2+}, Mn^{2+}, Cu^{2+}, and Co^{2+}). The values of T_m, T_c, and ΔH_m, which come from the polyethylene crystalline region, decrease with increasing neutralization in all the cation species. The values of T_i and ΔH_i, which come from the ionic crystallites, increase with neutraliza-

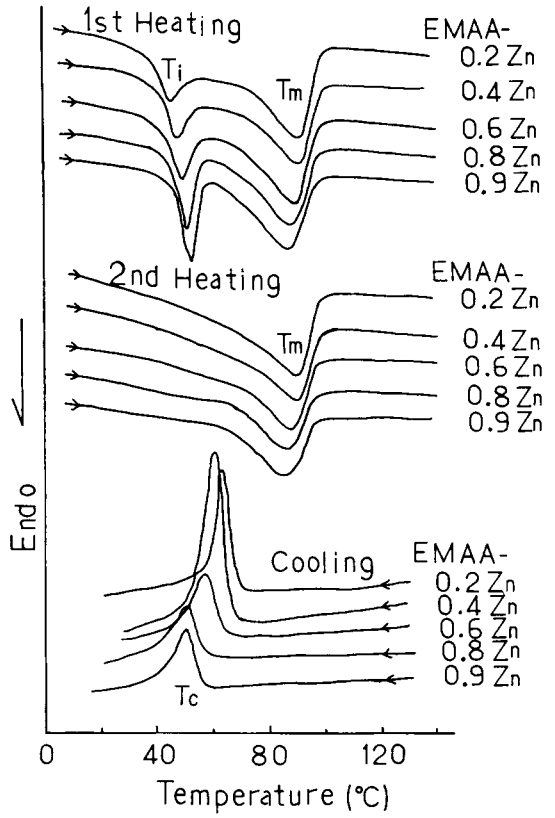

Figure 1 DSC thermograms vs. degree of neutralization for Zn ionomer.

tion. However, the values of T_i and ΔH_i for the Mg salt and the value of ΔH_i for the Na salt show a maxima in the plots.

It is noted that the changes in the thermal data with neutralization differ by the type of cation. The decreases of T_m, T_c, and ΔH_m with neutralization are considerably larger in the alkaline and alkaline earth metal salts than those in the transition metal salts. This phenomenon suggests that the stronger ionic interactions of both the alkaline and alkaline earth metal cations, which are shown in the MFR plots shown in the next paragraph, restrict the crystallization of polyethylene chains in the polymer matrix. The fact that the cation salts with the lower T_c show the lower ΔH_m supports this interpretation. The values of T_i and ΔH_i also differ according to the type of cation. The value of ΔH_i show a maximum or a plateau at a certain degree of neutralization in the alkaline and alkaline earth metal salts. This phenomenon is noticeable in the Na and Mg salts. The maximum is also shown in T_i for the Mg salt. On the other hand, the values of T_i and ΔH_i continuously increase with increasing neutralization in the transition metal salts. This difference in T_i and ΔH_i by the type of metal cation may suggest that the ordered structure of ionic crystallites differs by the type of cation. The maxima in ΔH_i may indicate that the orderliness inside the ionic crystallites de-

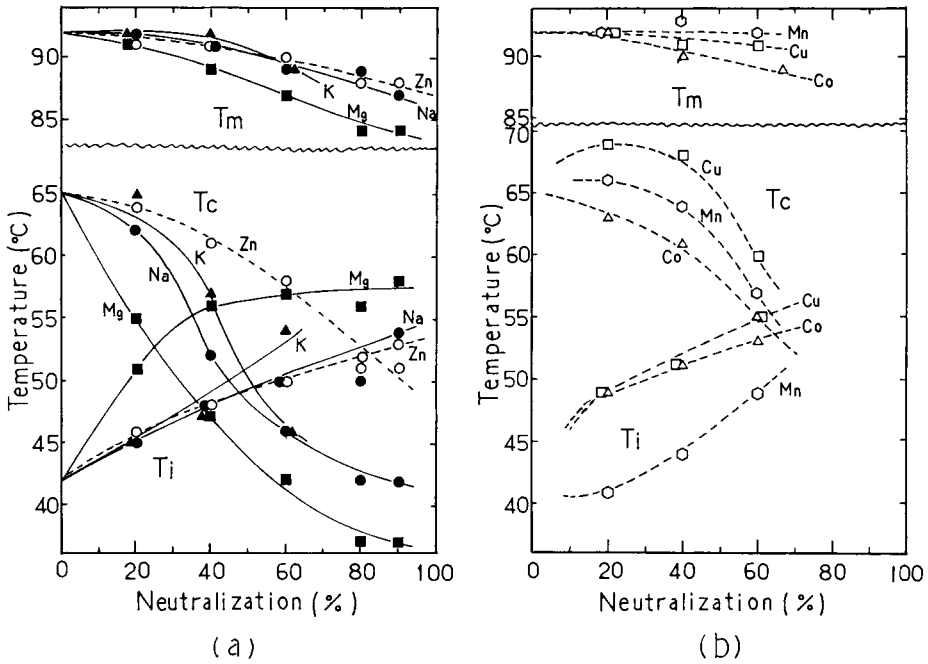

Figure 2 Changes in T_i, T_m, and T_c on DSC thermograms with degree of neutralization: (*a*) Na, Mg, K, and Zn ionomer. DSC thermograms were measured for the compression molded sheets aged for 2 months at 18–23°C. Cation type: (●) Na^+, (▲) K^+, (■) Mg^{2+}, (○) Zn^{2+}; (*b*) Cu, Mn and Co ionomer. DSC thermograms were measured for the pellet samples aged for 30 days at 18–23°C. Cation type: (□) Cu^{2+}, (○) Mn^{2+}, (△) Co^{2+}.

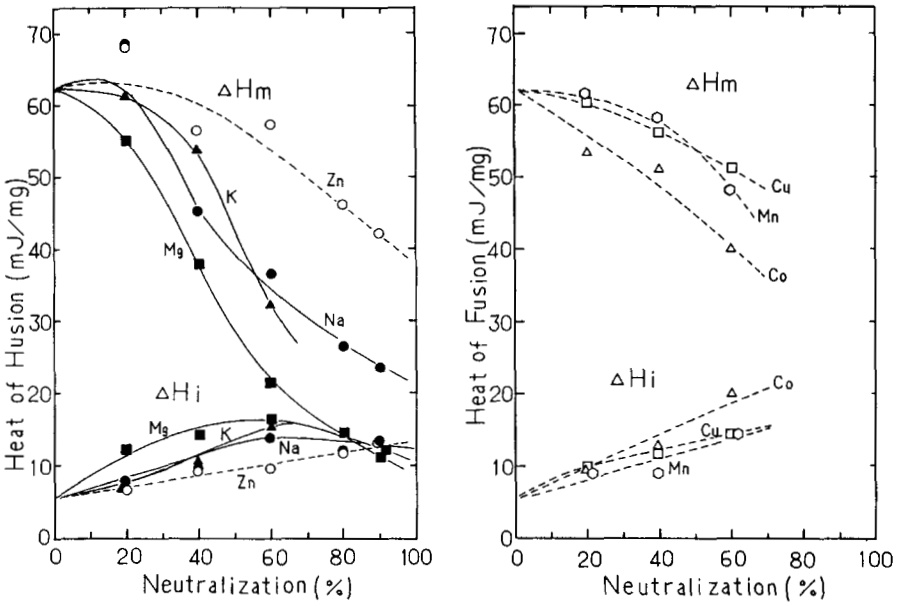

Figure 3 Changes in ΔH_i and ΔH_m on DSC thermograms with degree of neutralization: (a) Na, Mg, K and Zn ionomer. Cation type: (●) Na^+, (▲) K^+, (■) Mg^{2+}, (○) Zn^{2+}; (*b*) Cu, Mn, and Co ionomer. Cation type: (□) Cu^{2+}, (○) Mn^{2+}, (△) Co^{2+}.

creases above a critical degree of neutralization because the number of carboxylate ions or carboxyl groups per metal cation become unbalanced, as is later discussed in more detail.

These results show that the strength of ionic interactions and the degree of crystallization of ionic crystallites, which depend on the type of cation and the degree of neutralization, govern both the structure and the melting and crystallization properties of ionomers.

Melt Viscosity

Figure 4 shows the change of melt flow rate (MFR) with the degree of neutralization for all the samples. MFR decreases with increasing neutralization in all the samples. The decrease in MFR with neutralization, which means an increase in melt viscosity with neutralization, is larger for the alkaline and alkaline earth metal salts (denoted by solid lines) than for the transition metal salts (denoted by dotted lines). This result indicates that the ionic interactions in ionomer are larger with the alkaline and alkaline earth metal cations than with the transition metal cations in the molten state.

Stiffness (Bending Modulus)

Figure 5 shows how the stiffness changes with neutralization for Na, K, Mg, and Zn ionomers and also

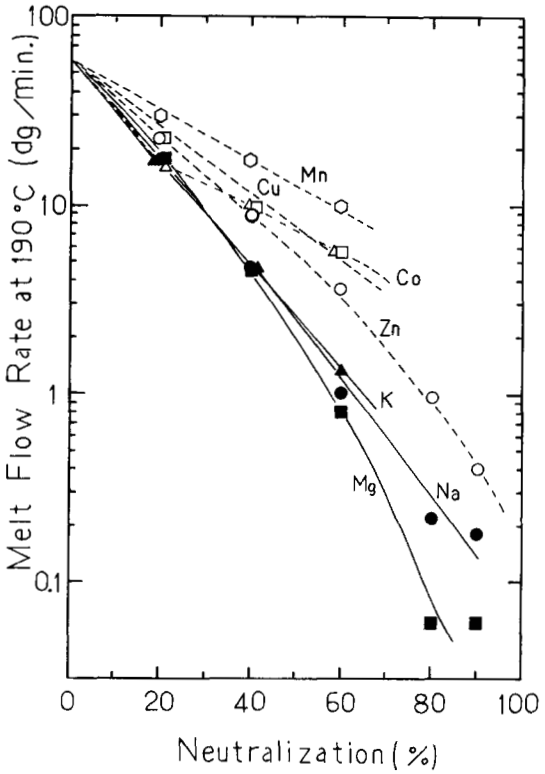

Figure 4 Comparison of the change in melt flow rate with degree of neutralization among various metal cation types. Cation type: (●) Na^+, (▲) K^+, (■) Mg^{2+}, (○) Zn^{2+}, (△) Co^{2+}, (□) Cu^{2+}, (○) Mn^{2+}.

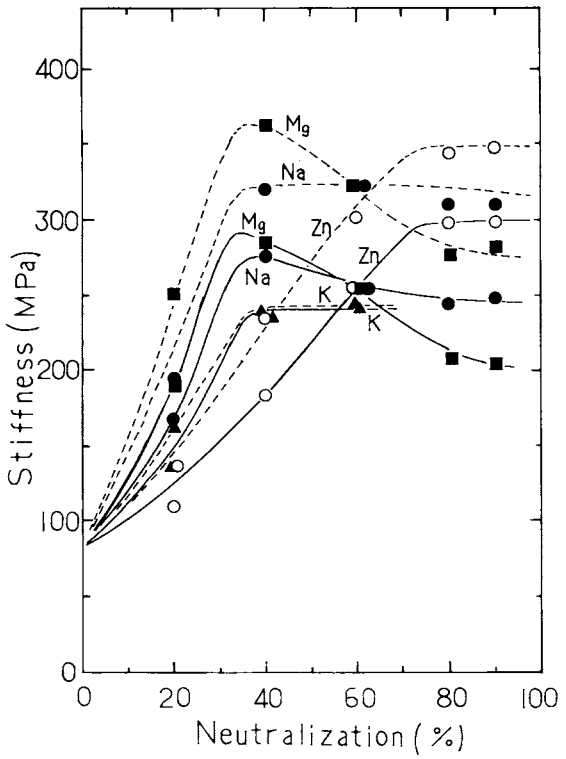

Figure 5 Stiffness vs. degree of neutralization for Na, Mg, K, and Zn ionomer. (——) Stiffness for the sheets aged for 2 months after molding. (------) Stiffness for the sheets aged for 3 months after molding. Cation type: (●) Na^+, (▲) K^+, (■) Mg^{2+}, (○) Zn^{2+}.

how the stiffness vs. neutralization plots change during aging after molding. Figure 6 shows how the stiffness vs. neutralization differ depending on the type of cation. In the two figures, we can easily find that the stiffness differs by the type of cation. The stiffness apparently shows a maximum at around 33% neutralization for the alkaline and alkaline earth metal salts. The stiffness steeply increases up to 33% neutralization, where it then makes plateaus or decreases with additional neutralization. On the other hand, in the transition metal salts, the stiffness increases monotonously with neutralization up to 60% neutralization. In the Zn salt, the increase in stiffness seems to saturate around 70% neutralization.

Such maxima in modulus at a specified degree of neutralization have been reported by several researchers. Rees et al.[11] found the stiffness peaked at 33% neutralization for the Na salts of several EMAAs with different MAA contents. Bonotto and Bonner[2,26] also reported the greatest modulus at 33% neutralization for the Na, K, Li, Ca, and Mg salts of poly(ethylene-*co*-acrylic acid) (EAA). They suggested that the ionomers show the maximum modulus when the ionic groups are packed to form the optimum spacing of the metal ions and the carboxyl groups in a relaxed structure. Wilson et al.[27] noted that alkaline ions have a tendency for sixfold or octahedral coordination, i.e., three carboxyl groups can be arranged in an octahedron around the metal ion. This structure could lead to a maximum in stiffness at 33% neutralization. They proposed that these coordinated ions have a tendency to cluster together and that this clustering imposes an order on the interconnecting hydrocarbon segments. They stated that it is the ordered chains that give rise to the scattering in SAXS analyses and not an ordered arrangement of the ionic aggregations. However, their interpretation contradicts the finding that the scattering exists in molten ionomers.[27]

Marx et al.[16] interpreted the changes in the wide-angle X-ray scattering behavior with composition in terms of the number of carboxyl groups per scattering site for the salts of EMAA and butadiene–methacrylic acid copolymers. They assumed that the scattering comes from scattering sites that contains

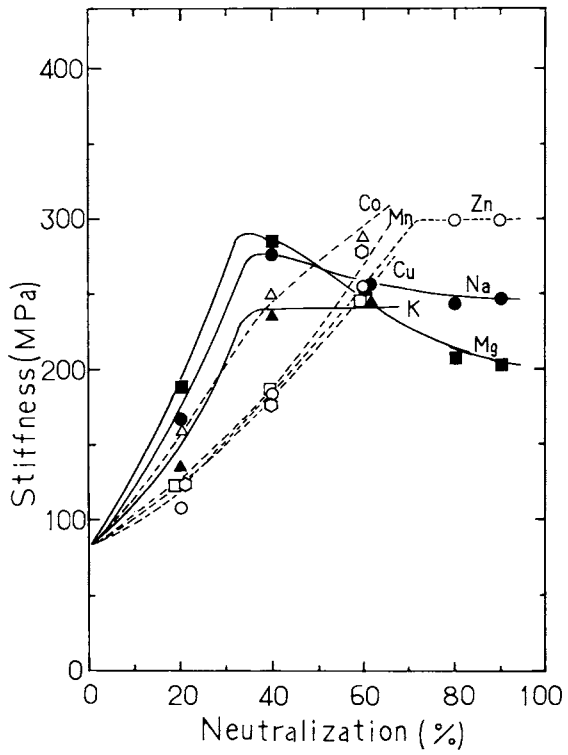

Figure 6 Comparison of the plots of stiffness vs. degree of neutralization among various cation types. Aging time after molding: 2 months—Na^+, Mg^{2+}, K^+ and Zn^{2+}; 9 days—Cu^{2+}, Mn^{2+}, Co^{2+}. (——) Alkaline and alkarine earth metals. (------) Transition metals. Cation type: (●) Na^+, (▲) K^+, (■) Mg^{2+}, (○) Zn^{2+}, (△) Co^{2+}, (□) Cu^{2+}, (○) Mn^{2+}.

one or more cations that are homogenously distributed throughout the amorphous phase. They showed that three carboxyl groups aggregate as trimers at the scattering sites in most sodium ionomers. They also observed that the carboxyl groups aggregate as trimers in the partially neutralized methacrylic acid and acitic acid by sodium hydroxide, which is quite similar to that observed in ionomers.

In our preceding studies,[24,25] we proposed an ordered structure of salt groups (ionic crystallites) inside the ionic clusters. The ordered structure of salt groups shows an order–disorder transition of first order near 330 K and predominantly governs the stiffness of ionomers.

Hirasawa et al.[28] showed that the stiffness shows a maximum at 67% neutralization for the Zn salts of EMAA, which is consistent with the present results. In this case, three carboxyl groups are estimated to be coordinated to a Zn^{2+} in the ionic clusters.

Recently, some evidence concerning the arrangement of ions inside the ionic clusters has been found by the use of new techniques: Extended X-ray absorption fine structure (EXAFS) results of Ding et al.[29] indicated the existence of some ordered structure in the ionic clusters for the Zn(II) salts of sulfonated polystylene. Register et al.[30] also indicated, by the use of EXAFS for the various metal salts of carboxyl-telechelic polyisoprene, that the orderliness in the ionic microdomains differs depending on the type of cation. The orderliness is higher for the metal cations that have a coordination number higher than the second shell. The metal salts with higher ionic orderliness show strain-hardening behavior.

Therefore, we should like to propose that the ordered structure of ionic salts in ethylene ionomers differs depending on the type of metal cations. Here, the number of carboxyl groups arranged around a metal cation is 3 for the alkaline metal salts, 6 for the alkaline earth metal salts, and 3 for the zinc salt. Figures 7(*a*) and (*b*) show the models of the ordered structure of ionic crystallites that we estimate for Na salt and Mg salt, respectively.

Below the neutralization level giving maximum stiffness, the slope in the stiffness–neutralization plots differs by the type of cation, which can be explained by both the strength of ionic interactions and the number of carboxyl groups arranged a metal cation. The plateau or the decreasing stiffness with neutralization above the maximum stiffness suggests that the excess metal cations would disturb the ordered structure of the ionic crystallites. This seems to explain the maximum of ΔH_i in the ΔH_i vs. neutralization plots for the Mg and Na salts shown in Figure 3(*a*).

Figures 8(*a*) and (*b*) show the plots of stiffness vs. heat of fusion of ionic crystallites (ΔH_i) for all ionomers used in this work. ΔH_i corresponds to the degree of crystallinity of ionic crystallites. The stiffness increases with increasing ΔH_i in all metal cation species independent of cation type. This clearly indicates that the stiffness of ionomer is closely connected with the existence and the degree of crystallinity of ionic crystallites, that is, the enhanced modulus upon neutralization comes from the formation of a rigid and ordered structure of ionic salt groups. These results correspond well with our preceding work.[25]

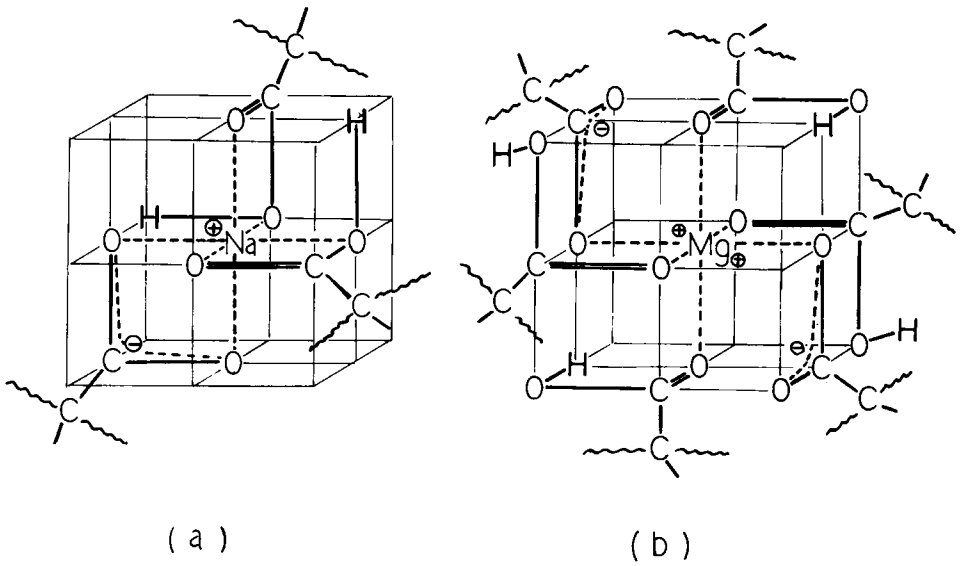

Figure 7 Ordered structure of ionic crystallites that are estimated for (*a*) Na salt, (*b*) Mg salt.

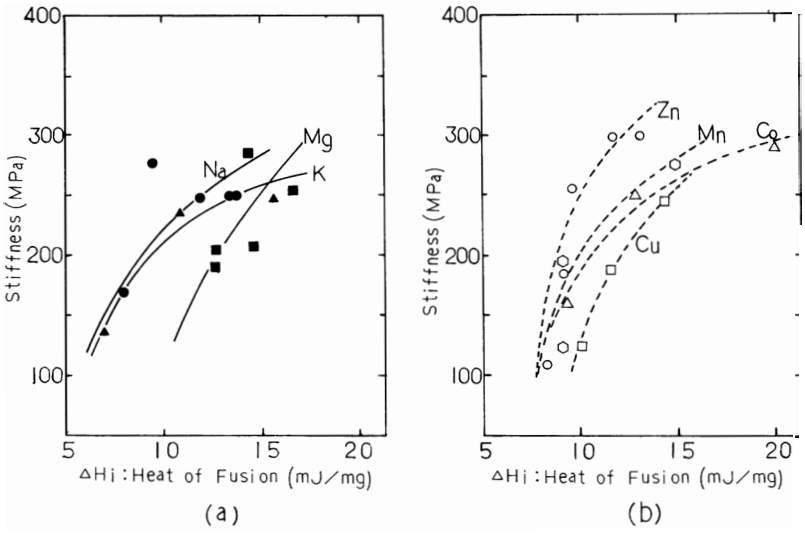

Figure 8 Stiffness vs. heat of fusion of ionic crystallites for all ionomers. Cation type (*a*): (●) Na^+, (▲) K^+, (■) Mg^{2+}; (*b*) (○) Zn^{2+}, (△) Co^{2+}, (□) Cu^{2+}, (○) Mn^{2+}.

Tensile Properties

Figures 9(*a*) and (*b*) show the plots of tensile properties vs. degree of neutralization for the Na, K, Mg, and Zn salts. With increasing neutralization, both the yield stress and the tensile strength increase, while the elongation decreases. These results are fundamentally consistent with those of other researchers.[2,10,11] However, we find a dependence of the yield stress behavior on the type of cation; the yield stress reaches a maximum or a plateau at a certain degree of neutralization for the alkaline and alkaline earth metal salts, whereas the yield stress continuously increases with neutralization for the Zn salt. These results are similar to those of the stiffness. Both stiffness and yield stress are measured under low strain, which means the physical structure such as ionic crystallites is not changed by the applied strain. Therefore, the ordered structure of ionic salts governs the stiffness and the yield stress, which leads to the difference in the stiffness and the yield stress according to the cation type. We

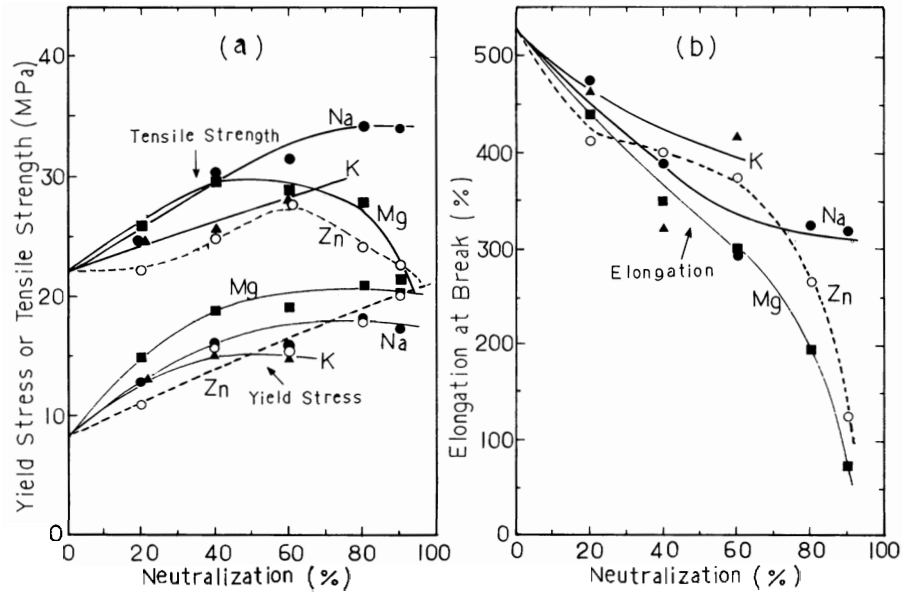

Figure 9 Tensile properties vs. degree of neutralization for Na, Mg, K, and Zn ionomer. (*a*) Yield stress and tensile strength, (*b*) elongation. Cation type: (●) Na^+, (▲) K^+, (■) Mg^{2+}, (○) Zn^{2+}.

observed an increase in the yield stress with aging,[31] similar to that in stiffness. This can be explained by the preceding interpretation.

Both the tensile strength and the elongation are strongly influenced by the valence of cation. Both monotonous increases in tensile strength and keeping of high elongation up to high neutralization are observed with monovalent metal salts. On the other hand, a drastic decrease in both the tensile strength and the elongation are observed above about 60% neutralization for divalent metal salts. Results similar to these have been reported by a few researchers. Murakami et al.[32] compared the tensile properties between Na^+ and Zn^{2+} salts of EAA and reported a drastic decrease in the elongation of Zn^{2+} ionomer, compared with that of Na^+. Bonotto and Bonner[2] also reported that the decrease in the elongation above 50% neutralization is larger for the Mg^{2+} and Ca^{2+} salts than for the Li^+, Na^+, and K^+ salts of EAA. These results suggest that the ordered structure of ionic salts does not affect these two properties. We observed no changes with aging in either tensile strength or elongation,[31] which supports the preceding interpretation. The large strain applied to measure these two properties will destroy the ordered structure of ionic salts, therefore, these two properties are not affected by the ionic crystallites.

Figure 10 shows the change of DSC curves by cold stretching for EMAA–0.6 Na. DSC thermograms in the first heating were compared between the ionomer sheet before stretching and that just after cold stretching by 300% elongation. The endothermic peak (T_m), corresponding to the melting of polyethylene crystallites, does not change so much by the stretching. On the other hand, the lower temperature peak (T_i), corresponding to the melting of ionic crystallites, decreases drastically both in peak temperature and peak area. This clearly indicates that the ordered structure of ionic crystallites is destroyed by the applied large strain, which supports that the ionic crystallites do not affect the large strain properties of ethylene ionomers.

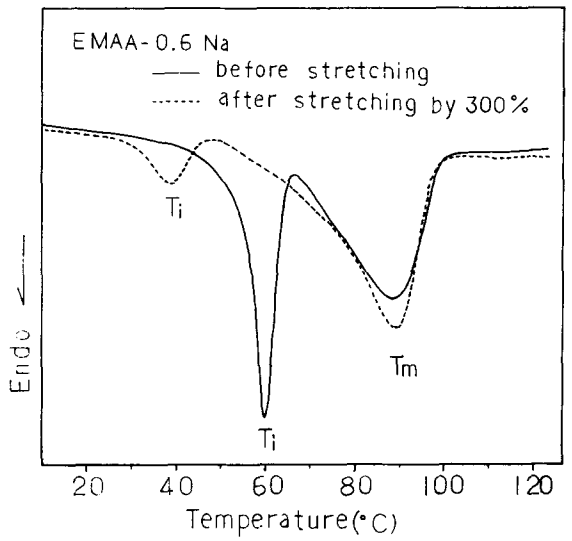

Figure 10 Change of DSC curves in the first heating by cold stretching. Sample: EMAA–0.6 Na, (——) before stretching, (------) shortly after stretching by 300%.

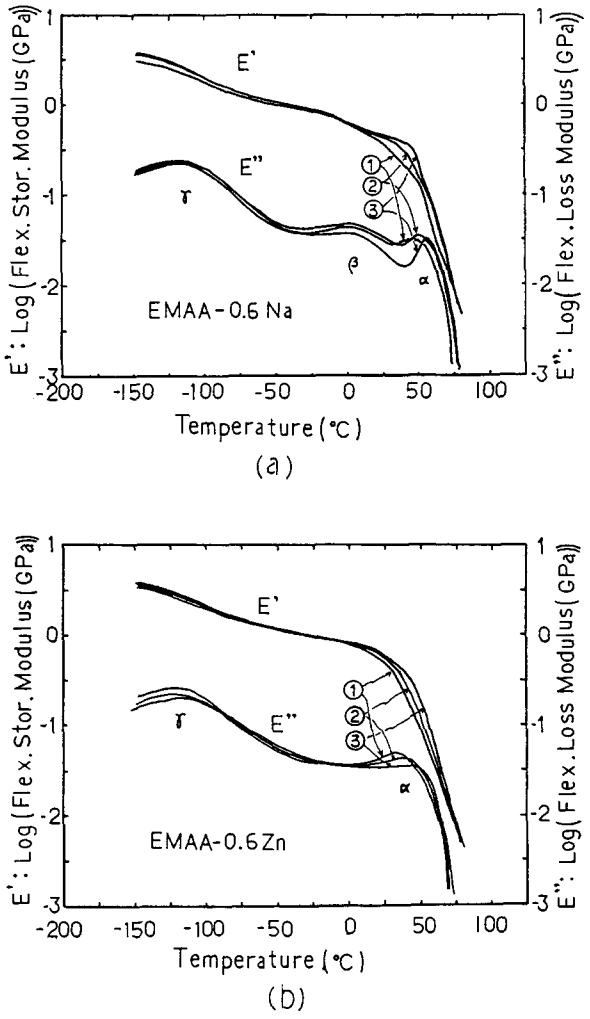

Figure 11 Change in dynamic mechanical properties with physical aging at room temperature. Aging duration after molding. ① 30 min, ② 3 days, ③ 2 months. (*a*) EMAA–0.6 Na, (*b*) EMAA–0.6 Zn.

Dynamic Mechanical Analyses

Figures 11(*a*) and (*b*) show how dynamic mechanical properties change with aging duration at room temperature after molding, for EMAA–0.6 Na and EMAA–0.6 Zn, respectively. A peak around 40–60°C

on the dynamic loss modulus–temperature curve (E'') (the peak is denoted by α), which was attributed to the melting of the ordered structure of ionic salt groups (ionic crystallites) in ionic clusters by our preceding work,[25] shifts to higher temperatures with aging duration in both Na and Zn salts. Accompanying this change, both the dynamic modulus (E') above 0°C and the bending point on E' curve also increase with aging. This indicates that the mechanisms underlying the modulus increase with aging are the formation and buildup of the ordered structure of ionic salt groups in a relaxation process.

Comparing the dynamic loss curves between Figures 11(a) and (b), we find a difference according to the type of cation. A dynamic loss peak around 0°C (denoted by β) is found in the Na salt but not in the Zn salt. This peak is assigned to a relaxation occurring in the amorphous branched polyethylene phase from which most of the ionic material has been excluded.[33] The position and intensity of this peak (β) does not change with aging. This indicates that almost all carboxyl and carboxylate groups of EMAA–0.6 Na are excluded from the amorphous phase and aggregate into ionic domains (ionic clusters) from the initial stage of molding from melt. This, in turn, suggests that the ionic aggregations (ionic clusters) exist in the molten state. In contrast, the separation of ionic groups is incomplete in EMAA–0.6 Zn; some of the carboxyl groups remain in the amorphous phase, while other carboxyl groups aggregate into ionic domains and form loose ionic clusters. This leads to the suppression of the β peak and the appearance of an α peak in the E'' curve of the Zn salt.

Figure 12(a) shows the dynamic mechanical curves for the alkaline and alkaline earth metal (K, Mg) salts and EMAA. In the temperature range above 0°C, only one dynamic loss peak (β') around 30°C is observed for EMAA. This peak was assigned to the relaxation in orderlike structure of associated carboxyl groups by our preceding work.[24] Upon neutralization by K^+ and Mg^{2+}, this peak is separated into two peaks, an α peak around 60°C and a β peak around 0°C. The assignments of the two peaks are the same as those shown for EMAA–0.6 Na in Figure 11(a). This indicates again that the microphase separation of ionic salt groups is almost complete in the alkaline and alkaline earth metal salts. Figure 12(b) shows also the dynamic mechanical curves of the transition metal salts (Cu, Mn, Co). In this figure, only one dynamic loss peak (α) is observed around 50–60°C for each ionomer in the temperature range above 0°C, as is observed for EMAA–0.6 Zn in Figure 11(b). There are no peaks or very small peaks on E'' curves around 0°C. This also indicates

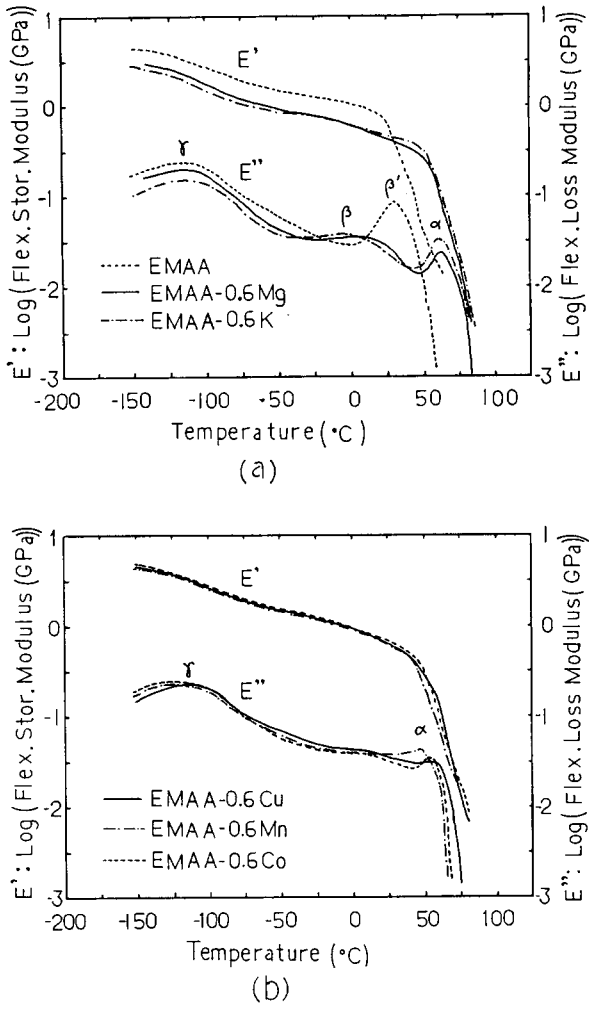

Figure 12 Temperature dependence of the dynamic mechanical properties. (a) EMAA, EMAA–0.6 Mg, and EMAA–0.6 K aged for 2 months after molding; (b) EMAA–0.6 Cu, EMAA–0.6 Mn, and EMAA–0.6 Co aged for 4 months after molding.

that the microphase separation of ionic salt groups is incomplete even at 60% neutralization for the transition metal salts. Abe et al.[34] showed that no distinct β peaks were found on dynamic mechanical loss curves for the Cu(II), Mn(II), and Ni(II) salts of EAA up to 70% neutralization. We also observed no clear β peak in the E'' curve for EMAA–0.8 Zn. However, we found a clear β peak around 10°C for excessively neutralized Zn(II) salt of EMAA (3.1 mol % MAA).[31] Therefore, it would be possible for transition metal ionomers to form regions of completely microphase-separated ionic salts, but it would be confined to very high neutralization levels.

The differences discussed for the dynamic mechanical properties according to the type of metal cation probably comes from the difference in the

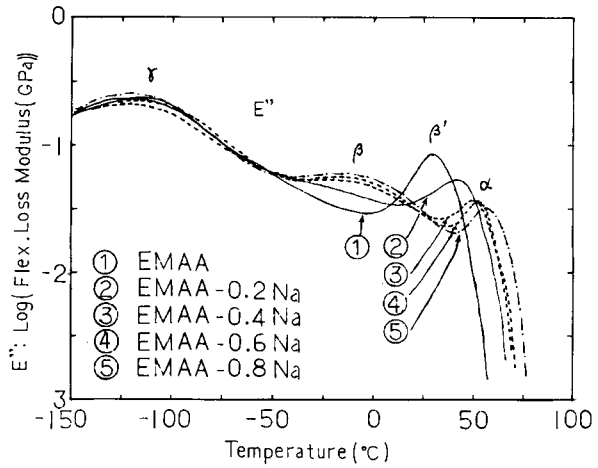

Figure 13 Temperature dependence of dynamic loss modules vs. neutralization for the EMAA–xNa system.

number of carboxyl groups arranged per metal cation. Three carboxyl or carboxylate groups arranged per metal cation (monovalent alkaline and alkaline earth metal salts) would result in almost all carboxyl groups aggregating into ionic domains and forming complete microphase separation at 33% neutralization. However, for the transition metal salts, the complete separation of the carboxyl groups from amorphous phase is not attained except at very high neutralization, because the number of carboxyl groups arranged around a metal cation is small.

Figure 13 denotes the change of dynamic loss modulus curves with neutralization for the EMAA–x-Na system. The β peak around 0°C is not seen for EMAA and EMAA–0.2 Na. But it appears for EMAA–0.4 Na and about 40% neutralization. This indicates that the microphase separation of ionic aggregates come to completion at the neutralization between 20 and 40% for the Na salts. Results similar to this are obtained for the K and Mg salts. These support the preceding interpretation.

Thus, we conclude that the ordered structure of the ionic crystallites govern the modulus and the microphase separation of ionic aggregates in ethylene ionomers.

REFERENCES

1. R. Longworth and D. J. Vaughan, *Nature,* **218,** 85 (1968).
2. S. Bonotto and E. F. Bonner, *Macromolecules,* **1,** 510 (1968).
3. E. Eisenberg, *Macromolecules,* **3**(2), 147 (1970).
4. L. Holliday, Ed., *Ionic Polymer,* Applied Science, London, 1975.
5. A. Eisenberg and M. King, Eds., *Ion-Containing Polymers, Polymer Physics,* Vol. 2, Academic Press, New York, 1977.
6. W. J. MacKnight and T. R. Earnest, *J. Polym. Sci., Macromol., Rev.,* **16,** 41 (1981).
7. A. D. Wilson and H. J. Prosser, Eds., *Development in Ionic Polymers,* Vol. 1, Applied Science, London, 1983.
8. M. Pineri and E. Eisenberg, Eds., *Structure and Properties of Ionomers,* NATO ASI Series, D. Reidel, Dordrecht, 1987.
9. U. S. Patent 3,264,272 (1963) (to E. I. DuPont Co. Inc.).
10. R. W. Rees and D. J. Vaughan, *ACS Polym. Preprints,* **6,** 287 (1965).
11. R. W. Rees and D. J. Vaughan, *ACS Polym. Preprints,* **6,** 296 (1965).
12. R. Longworth and F. C. Wilson, in *Ionic Polymer,* L. Holliday, Ed., Applied Science, London, 1975, pp. 164–169.
13. W. J. MacKnight, W. P. Taggart, and L. M. Mckenna, *J. Polym. Sci., Symp.,* **46,** 83 (1974).
14. Y. Tsujitai, S. L. Hsu, and W. J. MacKnight, *Macromolecules,* **14,** 1824 (1981).
15. M. Kohzaki, Y. Tsujita, A. Takizawa, and T. Kinoshita, *J. Appl. Polym. Sci.,* **33,** 2393 (1987).
16. C. L. Marx, D. F. Caulifield, and S. L. Cooper, *Macromolecules,* **6,** 344 (1973).
17. W. J. MacKnight, W. P. Taggart, and R. S. Stein, *J. Polym. Sci., Polym. Symp. Ed.,* **45,** 113 (1974).
18. M. Pineri, C. Meyer, A. M. Levelut, and M. Lumbert, *J. Polym. Sci., Polym. Phys. Ed.,* **12,** 115 (1974).
19. T. R. Earnest, Jr., J. S. Higgins, D. L. Handlin, and W. J. MacKnight, *Macromolecules,* **14,** 192 (1981).
20. M. Fujimura, T. Hashimoto, and H. Kawai, *Macromolecules,* **15,** 136 (1982).
21. D. J. Yarusso and S. L. Cooper, *Macromolecules,* **16,** 1871 (1983).
22. W. C. Forsman, *Macromolecules,* **15,** 1032 (1982).
23. B. Dreyfus, *Macromolecules,* **18,** 284 (1985).
24. K. Tadano, E. Hirasawa, H. Yamamoto, and S. Yano, *Macromolecules,* **22,** 226 (1989).
25. E. Hirasawa, Y. Yamamoto, K. Tadano, and S. Yano, *Macromolecules,* **22,** 2276 (1989).
26. S. Bonotto and E. F. Bonner, *ACS Polym. Preprints,* **9,** 537 (1968).
27. F. C. Wilson, R. W. Longworth, and D. J. Vaughan, *ACS Polym. Preprints,* **9,** 505 (1968).
28. E. Hirasawa and R. Ishimoto, *J. Adhesion Soc. Jpn.,* **18,** 247 (1982).
29. Y. S. Ding, D. J. Yarusso, H. K. D. Pan, and S. L. Cooper, *J. Appl. Phys.,* **56,** 2396 (1984).
30. R. A. Register, M. Foucart, R. Jerome, Y. S. Ding, and S. L. Cooper, *Macromolecules,* **21,** 1009 (1988).
31. E. Hirasawa, unpublished results.
32. J. Murakami, H. Ohara, and T. Yoshiki, *Kobunshi Ronbunshu,* **36,** 73 (1979).
33. P. J. Phillipes and W. J. MacKnight, *J. Polym., Sci.,* Part A-2, **8,** 727 (1970).
34. Y. Abe, S. Kayukawa, R. Sakamoto, and S. Yano, *Colloid Polym. Sci.,* **260,** 319 (1982).

Received March 29, 1989
Accepted March 21, 1990